Spin Crossover

DOI: 10.1002/ange.201107116

Crystallographic Evidence for Reversible Symmetry Breaking in a Spin-Crossover d^7 Cobalt(II) Coordination Polymer**

Kishalay Bhar, Sumitava Khan, José Sánchez Costa, Joan Ribas, Olivier Roubeau, Partha Mitra, and Barindra Kumar Ghosh**

In memory of Andres Goeta

An amazing example of bistability in molecular systems is given by spin crossover (SCO) materials.[1,2] These materials can be switched reversibly from a high-spin (HS) to a low-spin (LS) electronic state by applying an external perturbation, such as temperature, pressure, magnetic field, or light.[3] The SCO phenomenon occurs in a variety of d^4–d^7 transition-metal compounds. Fe^{II}[4] and Fe^{III}[5] have been by far the most studied metal ions in SCO, which is primarily due to their bistability features showing abrupt spin transition with hysteresis loops. Less attention has been paid to Co^{II}, perhaps owing to more gradual transitions. This d^7 ion may experience a change between $S = 1/2$ and $S = 3/2$ electronic states involving the transfer of one electron causing an appreciable difference in the coordination bond distances of about 0.10 Å.[6,7]

An important breakthrough in the SCO field is the application of polymeric systems to improve interactions between metal centers.[8] 1D polymers of the general type $[Fe(4\text{-R-}1,2,4\text{-triazole})_3]^{2+}$ (R = H, NH_2, and CH_2CH_2OH) are one of the most remarkable examples that show bistability with a hysteresis loop at room temperature. This polymer SCO system was the first tested as a memory device.[9,10]

Subtle information on effective SCO systems has been gained with the development of such characterization techniques as the X-ray diffraction; indeed, using this technique it has been illustrated that intermolecular interactions play a major role during such transition, and also that in some cases the transition may be accompanied with symmetry-breaking in the crystal structure. Remarkable examples of such phenonenon have been found in a few Fe^{II} compounds[11,12] and recently in a Fe^{III} complex.[13]

Herein we present the synthesis, structure, and magnetic and thermal properties of a Co^{II} 1D SCO polymer, $[Co(enbzpy)(dca)]_n(ClO_4)_n$ (**1**; enbzpy = *N*,*N*′-bis(2-pyridinylbenzylidene)ethane-1,2-diamine, dca = dicyanamide), which shows a reversible crystallographic symmetry-breaking. Compound **1** was formed in an MeOH solution containing a 1:1:1 mixture of $Co(ClO_4)_2\cdot 6H_2O$, enbzpy, and Na(dca). Single-crystal X-ray structures of **1** were determined at 296 K ($\mathbf{1}^{RT}$) and 100 K ($\mathbf{1}^{LT}$). Compound $\mathbf{1}^{RT}$ crystallizes in the monoclinic space group $P2_1/c$ (Supporting Information, Table S1); the coordination environment of the Co^{II} ion is a distorted octahedron with a CoN_6 chromophore, consisting of four equatorial N atoms of the Schiff base (enbzpy) and two axial nitrile N atoms of two different $\mu_{1,5}$ dca bridges that connect adjacent metal centers forming an infinite 1D chain. Co–N distances lie in the range 2.023–2.136 Å with an average value d_{av}(Co–N) of 2.08 Å, which is characteristic of Co^{II} HS systems.[14] The intra-chain Co1···Co1 separation is 8.57 Å. The central nitrogen atom of the $\mu_{1,5}$-dca bridge is disordered over two positions (Figure 1), forming a $\mu_{1,5}$-dca N6–N7-

[*] K. Bhar, S. Khan, Prof. B. K. Ghosh
Department of Chemistry, The University of Burdwan
Burdwan 713 104 (India)
E-mail: barin_1@yahoo.co.uk
Dr. J. S. Costa, Prof. J. Ribas
Departament de Química Inorgànica, Universitat de Barcelona
Diagonal, 645, 08028 Barcelona (Spain)
E-mail: josesanchezcosta@gmail.com
Dr. O. Roubeau
Instituto de Ciencia de Materiales de Aragón (ICMA)
CSIC—Universidad de Zaragoza
50009 Zaragoza (Spain)
P. Mitra
Department of Inorganic Chemistry, Indian Association for the Cultivation of Science
Kolkata 700 032 (India)

[**] This work was supported by the DST and CSIR, India. J.S.C. thanks the Spanish MICINN through CTQ2009-06959 for the research fellowship "Juan de la Cierva" (18-08-463B-750). J.R. also thanks the Spanish MICINN through CTQ2009-07264.

Supporting information for this article is available on the WWW under http://dx.doi.org/10.1002/anie.201107116.

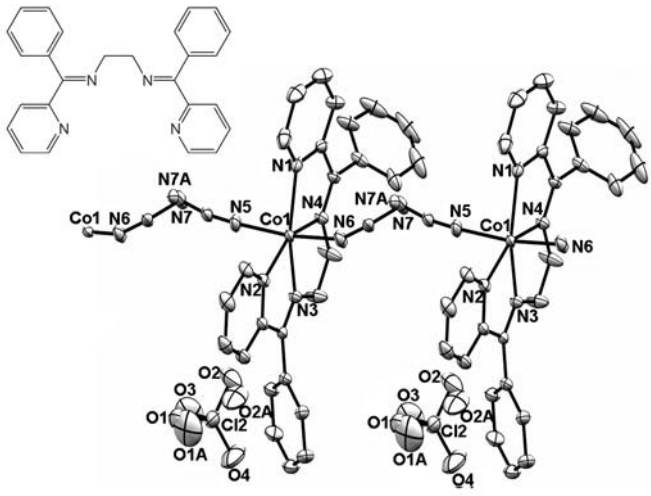

Figure 1. An ORTEP representation of a segment of the 1D chain along the *b* axis in $\mathbf{1}^{RT}$ with HS Co^{II}. Ellipsoids set at 30% probability; hydrogen atoms omitted for clarity. Inset: The enbzpy ligand.

(N7A)–N5 bridge angle of 133.49/133.01° (Supporting Information). The remaining crystal volume is occupied by a disordered ClO_4^- anion.

In the crystal packing of 1D chains of $\mathbf{1}^{RT}$, the aromatic rings in enbzpy and ClO_4^- are connected through weak C–H···O hydrogen bonds and C–H···π and π···π interactions (Supporting Information, Tables S2 and S3) with the neighboring enbzpy unit affording a superstructure. The adjacent 1D chains in $\mathbf{1}^{RT}$ are engaged in C–H···π interactions involving the H atom (H21) of a phenyl ring and the π cloud of a pyridine ring (defined as Cg8, see the Supporting Information) of two closest enbzpy ligands. Furthermore, they are connected through cooperative C–H···O hydrogen bonds (Supporting Information, Figure S1) between ClO_4^- counterions embedded between those chains and hydrogen atoms of enbzpy, leading to a 3D network structure. The packing is further stabilized through C–H···N interactions involving the hydrogen of a phenyl ring (H23) and nitrogen atoms (N6) of the dca bridge along with π···π interactions of the nearest phenyl rings (Cg9) in enbzpy ligands.

The magnetic susceptibilities for **1** were determined over the temperature range 2–300 K applying a constant field of 0.5 T, in both cooling and warming modes (Figure 2). The room-temperature $\chi_M T$ value of 2.43 $cm^3 mol^{-1} K$ is greater than that expected for a d^7 mononuclear cobalt(II) ($S = 3/2$, $\chi_M T = 1.87$ $cm^3 mol^{-1} K$), which is presumably due to a large first-order orbital angular momentum contribution to the magnetic moment. On cooling, $\chi_M T$ decreases slightly until 191 K and drops abruptly to reach a value of 1.65 $cm^3 mol^{-1} K$ at about 171 K. This remains almost constant down to 100 K and again decreases to attain a value of 1.41 $cm^3 mol^{-1} K$. Below 10 K, the $\chi_M T$ value increases reaching a maximum of 1.60 $cm^3 mol^{-1} K$. The value of $\chi_M T$ below the abrupt drop around 190 K can be reasonably ascribed to two Co^{II} HS atoms and two Co^{II} LS (expected = 1.4 $cm^3 mol^{-1} K$), in agreement with structural parameters (see below). Surprisingly for this 1D Co^{II} SCO system, the transition occurs with a small hysteresis loop of 3 K width (Figure 2, inset). This behavior suggests an efficient cooperative effect both among adjacent Co^{II} centers along the 1D supramolecular chains and between chains through interchain interactions. Furthermore, the hysteresis loop was confirmed by calorimetric studies (see

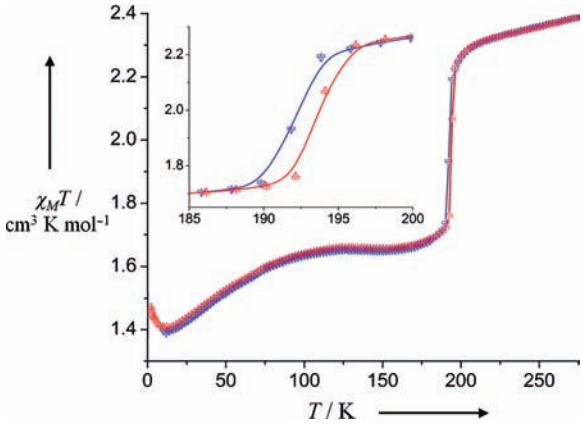

Figure 2. $\chi_M T$ versus T plot for **1** illustrating the abrupt SCO transition with a small hysteresis loop of 3 K (inset). Blue represents the magnetic data collected in cooling mode and red in warming mode.

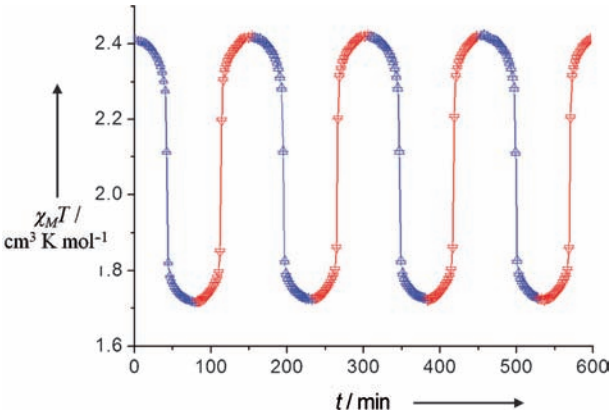

Figure 3. $\chi_M T$ versus time over four thermal cycles in the temperature range 227–160 K. The HS→LS transition is represented in blue and the LS→HS in red.

below) and reproduced over four times in the 227–160 K temperature range, thus showing that **1** is an example of a Co^{II} polymer with a robust SCO behavior (Figure 3).

In view of the magnetic behavior, we decided to resolve the structure of **1** at low temperature. Compound $\mathbf{1}^{LT}$ crystallizes in a low-symmetry space group, the triclinic $P\bar{1}$ (Experimental Section) with similar a and c cell lengths as for $\mathbf{1}^{RT}$, and a doubling of the b axis and cell volume (see crystal data). The asymmetric unit contains four crystallographically different Co^{II} centers (Co1A, Co1B, Co2A, and Co2B). The coordination environment of the metal is analogous to that observed in $\mathbf{1}^{RT}$. The average Co–N distances (Supporting Information, Table S1) are now d_{av}(Co1A–N) 2.108 Å, d_{av}(Co2A–N) 2.015 Å, d_{av}(Co1B–N) 2.111 Å, and d_{av}(Co2B–N) 2.016 Å, thus indicating that Co1A and Co1B are in the HS state, whereas Co2A and Co2B, are in the LS state.[14] This spin transition in the crystal is illustrated in Figure 4. The intrachain distances observed in chain A are Co1A···Co2A/Co2A···Co1A 8.673/8.573 Å, and in B they are Co1B···Co2B/Co2B···Co1B 8.639/8.581 Å. The angle formed by the two crystallographically independent $\mu_{1,5}$-dca bridges for chain A are N5-N6-N7 127.22° and N12-N13-N14 131.63°, and for chain B they are N5-N6-N7 128.33° and N12-N13-N14 131.61° (Supporting Information, Figure S4). In both cases the angles formed by the $\mu_{1,5}$-dca are smaller compared to those in $\mathbf{1}^{RT}$.

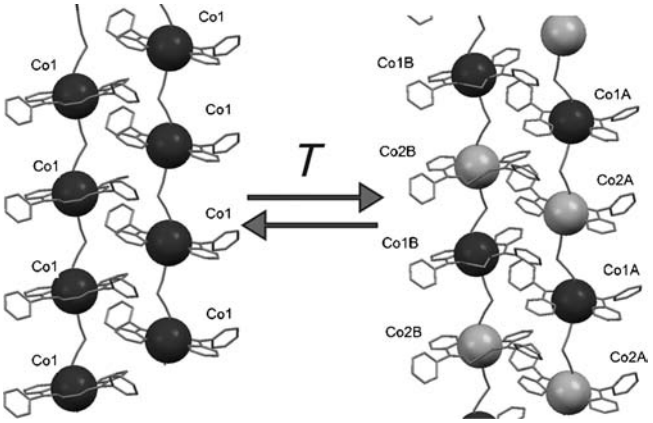

Figure 4. View of the 1D chains evolution during the SCO process along the c axis. HS Co dark gray, LS light gray.

In crystalline state, the single $\mu_{1,5}$-dca bridged spin-active Co^{II} centers in **1** are organized on a global basis through different intermolecular forces, such as C–H···π interactions, π···π stacking, and hydrogen bonding. These noncovalent interactions play a pivotal role as information transmitters among the active metal(II) centers throughout the whole network.

Crystal packings of $\mathbf{1}^{\mathbf{RT}}$ and $\mathbf{1}^{\mathbf{LT}}$ show that the pattern of intermolecular interactions (Supporting Information, Tables S2–S5) are similar; however, the degree of interactions increases substantially in $\mathbf{1}^{\mathbf{LT}}$. In $\mathbf{1}^{\mathbf{LT}}$, two independent 1D chains (Co1A···Co2A and Co1B···Co2B) are stacked alternating parallel to the *ab* plane (Supporting Information, Figure S2) through multiple C–H···N hydrogen bonds involving N atoms (N7B, N13B and N14B) of the dca bridges from chain B (Co1B/Co2B) and H atoms (H11A, H32A and H39A) of enbzpy from chain A (Co1A/Co2A).

These 2D sheets are further stabilized through C–H···π interactions (Supporting Information, Figure S3, Table S4) among chains A and B. Multiple C–H···O hydrogen bonds to the perchlorate counterions embedded between those sheets and weak π···π interaction between two adjacent B chains (Co1B···Co2B) along *c* axis also strengthen these supramolecular interactions, affording a 3D network (Supporting Information, Tables S4, S5). The broader array of interactions involving the dca in $\mathbf{1}^{\mathbf{LT}}$ is symptomatic of an internal reorganization in the polymeric chain without loss of crystallinity.

An appealing phenomenon involving the ClO_4^- counterions and the $\mu_{1,5}$-dca bridged occurs during the transition (Figure 5). The O10 (O10 and O10A) is involved in a supramolecular contact with one of the dicyanamide group O10···C56A (3.235 Å) and O10A···C56A (3.048 Å), O10A···N13A (3.054 Å), with the adjacent dca ligand (N12A-C55A-N13A-C56A-N14A). This contact can be considered an anion–π interaction.[15] In fact, the reorientation of the perchlorate likely plays an important role in the occurrence of the small hysteresis loop[16] (inset in Figure 2).

Differential scanning calorimetry (DSC) measurements were performed to confirm the above observations. The raw DSC traces (Supporting Information, Figure S5) show very sharp peaks in both cooling and warming modes at temperatures similar to those observed in the magnetic measurements, and confirm the presence of a hysteresis of about 3 K width. This is reproducible over various temperature cycles. The excess enthalpy and entropy of the transition, derived from the excess heat capacity (Supporting Information, Figure S6), amount to 2.11 kJ mol^{-1} and 10.9 J mol^{-1} K^{-1}, respectively. Altogether, these calorimetric features are consistent with a cooperative first-order transition, in agreement with the observation of a crystallographic transition coupled with the spin crossover. In particular, the excess entropy is much larger than that expected from the electronic transition of half of the Co^{II} ions, and thus likely includes the contribution from the crystallographic transition, and a vibrational term possibly involving the ordering of the dicyanamide ion and intermolecular interactions.

Figure 5. The supramolecular anion–π interaction in $\mathbf{1}^{\mathbf{LT}}$ involving O10 of the disordered perchlorate unit and the π cloud of a dicyanamide bridge (N12A–C55A–N13A–C56A–N14A).

In summary, complex **1** is the first example of a symmetry-breaking spin transition for a Co^{II} SCO polymer where a rare abrupt HS↔LS transition is found. It is an unprecedented X-ray crystallographically characterized structural phase transition accompanied with sufficiently strong reorganization of the intermolecular interactions. The spin-inactive components, such as the ligand and the counterion, also play a dominant role in the spin transition through supramolecular contacts. Remarkably, the transition between both phases has been proved to be crystallographically reversible. A huge modification in the assemblage of the 1D chains has no repercussions in the reversibility of the symmetry-breaking abrupt spin crossover. DFT calculations are underway to better understand such symmetry-breaking SCO behavior associated with cooperativity and hysteresis in terms of electronic.

Experimental Section

Crystal data for $\mathbf{1}^{\mathbf{RT}}$: $C_{28}H_{22}N_7O_4ClCo$, $M_r = 614.91$, monoclinic, space group $P2_1/c$, crystal size $= 0.17 \times 0.13 \times 0.08$ mm^3, $a = 15.138(14)$, $b = 8.569(8)$, $c = 20.963(19)$ Å, $\beta = 91.546(12)°$, $V = 2718(4)$ Å^3, $Z = 4$, $\rho_{calcd} = 1.502$ g cm^{-1}; $T = 296(2)$ K, $\mu(Mo_{K\alpha}) = 0.779$ mm^{-1} ($\lambda = 0.71073$ Å); 38232 reflections measured, 8515 unique ($R_{int} = 0.073$), refinement converged to $R = 0.0664$, $wR(F^2)$ [$I > 2\sigma(I)$] $= 0.2029$, 397 parameters and 414 restraints, goodness of fit on $F^2 = 1.005$; max./min. residual electron density $= +0.661/-0.889$ e Å^{-3}. Crystal data for $\mathbf{1}^{\mathbf{LT}}$: $C_{56}H_{44}N_{14}O_8Cl_2Co_2$, $M_r = 1229.81$, triclinic, space group $P\bar{1}$, crystal size $= 0.17 \times 0.13 \times 0.08$ mm^3, $a = 15.294(4)$, $b = 17.195(4)$, $c = 22.068(6)$ Å, $\alpha = 68.124(4)$, $\beta = 89.466(4)$, $\gamma = 88.942(4)°$, $V = 5384(2)$ Å^3, $Z = 4$, $\rho_{calcd} = 1.517$ g cm^{-1}; $T = 100.0(1)$ K, $\mu(Mo_{K\alpha}) = 0.786$ mm^{-1}(λ=0.71073 Å); 59801 reflections measured, 22918 unique ($R_{int} = 0.083$), refinement converged to $R = 0.1354$, $wR(F^2) = 0.3962$ [$I > 2\sigma(I)$], 1486 parameters and 2464 restraints, goodness of fit on $F^2 = 1.037$; max./min. residual electron density $= +4.517/-1.791$ e Å^{-3}. CCDC 833288 ($\mathbf{1}^{\mathbf{RT}}$) and 833289 ($\mathbf{1}^{\mathbf{LT}}$) contain the supplementary crystallographic data for this paper. These data can be obtained free of charge from The Cambridge Crystallographic Data Centre via www.ccdc.cam.ac.uk/data_request/cif.

Synthetic details, magnetic susceptibility measurements, DSC experiments, X-ray crystallographic analyses, crystallographic data including bond distances, bond angles, non-covalent interaction parameters (Tables S1–S5), and structures (Figure S1–S4) of $\mathbf{1}^{\mathbf{RT}}$ and $\mathbf{1}^{\mathbf{LT}}$ are available in the supporting information.

Received: October 7, 2011
Revised: December 5, 2011
Published online: January 23, 2012

Keywords: cobalt · coordination polymers · magnetic properties · spin crossover · symmetry breaking

[1] P. Gamez, J. S. Costa, M. Quesada, G. Aromí, *Dalton Trans.* **2009**, 7845 – 7853.
[2] A. Bousseksou, G. Molnár, L. Salmon, W. Nicolazzi, *Chem. Soc. Rev.* **2011**, *40*, 3313 – 3335.
[3] P. Gutlich, H. A. Goodwin in *Spin Crossover in Transition Metal Compounds I*, Springer, Berlin, **2004**, pp. 1 – 47.
[4] M. Halcrow, *Chem. Soc. Rev.* **2011**, *40*, 4119 – 4142.
[5] T. M. Ross, S. M. Neville, D. S. Innes, D. R. Turner, B. Moubaraki, K. S. Murray, *Dalton Trans.* **2010**, *39*, 149 – 159.
[6] S. Hayami, Y. Komatsu, T. Shimize, H. Kamihata, Y. H. Lee, *Coord. Chem. Rev.* **2011**, *255*, 1981 – 1990.
[7] G. Agustí, C. Bartual, V. Martinez, F. J. Muñoz-Lara, A. B. Gaspar, M. C. Muñoz, J. A. Real, *New J. Chem.* **2009**, *33*, 1262 – 1267.
[8] K. S. Murray, *Eur. J. Inorg. Chem.* **2008**, 3101 – 3121.
[9] O. Kahn, C. J. Martinez, *Science* **1998**, *279*, 44 – 48.
[10] J. F. Létard, P. Guionneau, L. Goux-Capes in *Spin Crossover in Transition Metal Compounds III*, Springer, Berlin, **2004**, pp. 221 – 249.
[11] S. Bonnet, M. A. Siegler, J. S. Costa, G. Molnár, A. Bousseksou, A. L. Spek, P. Gamez, J. Reedijk, *Chem. Commun.* **2008**, 5619 – 5621.
[12] N. Bréfuel, H. Watanabe, L. Toupet, J. Come, N. Matsumoto, E. Collet, K. Tanaka, J. P. Tuchagues, *Angew. Chem.* **2009**, *121*, 9468 – 9471; *Angew. Chem. Int. Ed.* **2009**, *48*, 9304 – 9307.
[13] M. Griffin, S. Shakespeare, H. J. Shepherd, C. J. Harding, J.-F. Létard, C. Desplanches, A. E. Goeta, J. A. K. Howard, A. K. Powell, V. Mereacre, Y. Garcia, A. D. Naik, H. Müller-Bunz, G. G. Morgan, *Angew. Chem.* **2011**, *123*, 926 – 930; *Angew. Chem. Int. Ed.* **2011**, *50*, 896 – 900.
[14] G. Juhász, R. Matsuda, S. Kanegawa, K. Inoue, O. Sato, K. Yoshizawa, *J. Am. Chem. Soc.* **2009**, *131*, 4560 – 4561.
[15] T. J. Mooibroek, C. A. Black, P. Gamez, J. Reedijk, *Cryst. Growth Des.* **2008**, *8*, 1082 – 1093.
[16] G. A. Craig, J. S. Costa, O. Roubeau, T. S. Teat, G. Aromí, *Chem. Eur. J.* **2011**, *17*, 3120 – 3127.

